Inorganic Chemistry Communications 54 (2015) 54–56

Contents lists available at ScienceDirect

Inorganic Chemistry Communications

journal homepage: www.elsevier.com/locate/inoche

Spillover enhanced hydrogen storage in Pt-doped MOF/graphene oxide composite produced via an impregnation method

Hu Zhou [a,b], Jun Zhang [c], Jian Zhang [c], Xiu-Fen Yan [c], Xiao-Ping Shen [d], Ai-Hua Yuan [c,*]

[a] School of Material Science and Engineering, Jiangsu University of Science and Technology, Zhenjiang 212003, China
[b] Siyang Diesel Engine Manufacturing Co., Ltd, Zhenjiang 212003, China
[c] School of Environmental and Chemical Engineering, Jiangsu University of Science and Technology, Zhenjiang 212003, China
[d] School of Chemistry and Chemical Engineering, Jiangsu University, Zhenjiang 212013, China

ARTICLE INFO

Article history:
Received 23 August 2014
Received in revised form 28 November 2014
Accepted 2 February 2015
Available online 3 February 2015

Keywords:
Hydrogen storage
MOFs
Graphene oxide
Platinum
Impregnation

ABSTRACT

Pt-doped MOF/graphene oxide (GO) composites were synthesized via a colloidal Pt nanoparticle (NP) incipient-wetness impregnation method for the first time. The composites Pt@HKUST-1/GO and Pt@ZIF-8/GO were characterized by X-ray diffraction, electron microscopy and gas adsorption. The hydrogen uptakes of both composites at 298 K and 860 mm Hg were enhanced by a factor of 3.6 or 4.1 compared to MOFs, although Pt NPs were obviously aggregated throughout MOF/GO networks. This significant enhancement is mainly attributed to the combination of high porosities of MOF/GO supports and hydrogen spillover mechanism, in which Pt NPs and MOF/GO act as dissociation source and receptor, respectively.

Hydrogen is one of the most promising candidates as a renewable, environmentally friendly energy carrier. Metal–organic frameworks (MOFs) have been proven to be excellent candidates for hydrogen storage, due to their merits of high crystallinity, purity, adjustable high porosity and controllable structural characteristics [1]. However, hydrogen uptakes of MOFs decrease dramatically upon elevating temperatures, because the storage of H_2 molecules relies on weak physisorption, and thus must be performed at extremely low temperatures. Recently, the spillover effect for enhanced uptakes at 298 K on absorbents has attracted much attention from the viewpoint of practical applications [2,3]. Hydrogen spillover is defined as the dissociative chemisorptions of H_2 on metals and the subsequent migration of atomic H onto the surface of support [4]. Significantly enhanced hydrogen storage capacities at 298 K were achieved compared to MOFs by mixing Pt/AC catalysts with MOFs [5–9].

The feature of supports and doping method are important factors affecting spillover hydrogen uptakes [2]. Bandosz and other groups have constructed MOF/graphene oxide (GO) composites [10–16], and the synergistic effect on porosity and chemistry of MOF/GO resulted in an obvious improvement in H_2 uptakes. In this paper, we tried to incorporate Pt nanoparticles (NPs) into MOF/GO (MOF: HKUST-1, ZIF-8), and dramatically enhanced capacities were achieved at 298 K. To our knowledge, there were only two reports of NPs@MOF/GO so far [17,18], and this is the first example of a NP-doped MOF/GO system prepared by a colloidal NP incipient-wetness impregnation method.

GO and Pt NPs were prepared by a modified Hummers method [19] and using polyol reduction [20], respectively (Figs. S1, S2). HKUST-1 and ZIF-8 were obtained by reported methods [21,22]. HKUST-1/GO and ZIF-8/GO were prepared in the same procedure as MOFs except that an amount of GO was added to the mixture of MOF precursors before reaction. The GO consisted of 5 wt.% of the final material weight. The HKUST-1/GO sample was ground and then activated at 160 °C under vacuum for 24 h before loading. Pt NPs were dispersed in 1 mL ethanol, and the colloidal solution was added into a vial of 0.2 g HKUST-1/GO. The mixture was ultrasonicated for 15 min and dried at 60 °C. Before adsorption experiments, Pt@HKUST-1/GO was evacuated at 160 °C to remove residual solvents. Pt@ZIF-8/GO was obtained by following the same procedure. Pt contents in Pt@HKUST-1/GO and Pt@ZIF-8/GO were estimated to be ca. 1.19 wt.% and 0.98 wt.% by ICP analysis, respectively.

The XRD peak at $2\theta = 9.76°$ for GO can be assigned to the (0 0 1) crystal face (Fig. S3). The peaks of both MOFs matched well with those simulated from single crystal structural data [23,24], indicating the successful preparation of MOF. MOF/GO and Pt@MOF/GO exhibited similar patterns to MOFs, confirming that the framework of MOF was well preserved. The absence of peaks assigned to GO in supports and composites can be attributed to the low GO content, and/or the exfoliation/high dispersion of GO in mixture solution upon sonication during the preparation procedure [25]. Notably, the diffraction

* Corresponding author.
E-mail address: aihua.yuan@just.edu.cn (A.-H. Yuan).

http://dx.doi.org/10.1016/j.inoche.2015.02.001
1387-7003/

intensities of Pt@MOF/GO slightly decreased after loading Pt NPs due to the loss in crystallinity and/or structural distortion caused by the inclusion of Pt NPs. The peaks at around 40° and 46° in Pt@MOF/GO can be ascribed to the (1 1 1) and (2 0 0) crystal faces of Pt(0), respectively (Fig. S3 inset).

The color of Pt@MOF/GO changed darker than MOF/GO and MOFs (Fig. S4a), demonstrating the successful incorporation of GO and Pt NPs. HKUST-1 exhibits an octahedral crystalline shape (Fig. S4b). The layer feature with a few GO agglomerates for HKUST-1/GO and Pt@HKUST-1/GO is indicative of intercalations of GO and MOF [10,11]. Different from Pt@HKUST-1/GO, ZIF-8 crystals have a nanoscale size and are randomly dispersed on GO in ZIG-8/GO and Pt@ZIF-8/GO with a similar morphology and size with respect to ZIF-8.

It should be noted that large Pt NP aggregations were clearly observed throughout Pt@HKUST-1/GO (Fig. 1a). The average size of Pt NPs is ca. 3.6 nm, much larger than the pore size (0.9 nm × 0.9 nm) in the structure of HKUST-1 [23], indicating that Pt NPs were located on outer surfaces not into cavities of HKUST-1. ZIF-8 exhibited uniformly hexagonal morphology with the size of ca. 70–110 nm. Identical hexagonal morphology and particle size of ZIF-8 are found for ZIF-8/GO and Pt@ZIF-8/GO, in which ZIF-8 nanocrystals were homogeneously distributed with a few irregular GO sheets. The significant aggregation of Pt NPs was observed in Pt@ZIF-8/GO. Also, Pt NPs are located on GO, and external surface and edges of ZIF-8 since they are larger than pores of ZIF-8, which contains large cavities (1.16 nm of diameter) interconnected by narrow windows (0.34 nm of diameter) [24]. Element mapping images of Pt@MOF/GO further confirmed the obvious aggregation of Pt NPs in the micro/nano region (Fig. 1b). The incipient-wetness impregnation of our MOF/GO supports with colloidal Pt NPs may lead to a more heterogeneous dispersion of Pt particles including larger agglomerates outside, even low Pt loadings.

HKUST-1 and ZIF-8 show typical type-I isotherms (Fig. S5), and the BET value of HKUST-1 is 1131 $m^2 g^{-1}$ (Table S1), close to the reported value [26]. The value of 1142 $m^2 g^{-1}$ for ZIF-8 is higher than 962 $m^2 g^{-1}$ for nanoscale ZIF-8 [22], and lower than the highest value (1630 $m^2 g^{-1}$) reported for microscale ZIF-8 [24]. However, the value of ZIF-8/GO remains unchanged, while a slight loss was observed for HKUST-1/GO upon incorporation of GO. Notably, the measured BET value (1161 $m^2 g^{-1}$) for ZIF-8/GO is higher than the hypothetical one (1085 $m^2 g^{-1}$). The latter one was calculated assuming the physical mixture of ZIF-8 and GO alone, taking into account the percentage of each component. This result can be ascribed to the synergistic effect between ZIF-8 and GO, where the new pores were formed at the interface between GO layers and ZIF-8, as observed in other MOF/GO materials [10–12]. The BET value of Pt@HKUST-1/GO decreased dramatically compared to the slight decline for Pt@ZIF-8/GO. The significant loss for Pt@HKUST-1/GO can be ascribed to large cavities in MOF blocked by aggregated Pt NPs. The negligible loss for Pt@ZIF-8/GO relative to ZIF-8 can be due to the synergistic effect between ZIF-8 and GO, and that aggregated Pt NPs are located on outer surfaces and edges of ZIF-8 not in cages.

As expected, MOFs and MOF/GO exhibited very low hydrogen uptakes at 298 K (Fig. 2) due to the weak van der Waals interactions between MOFs and H_2. However, a pronounced enhancement for Pt@HKUST-1/GO and Pt@ZIF-8/GO was observed at 298 K, with factors of 3.6 and 4.1 compared to MOFs, respectively, although ad- and desorption curves for both composites are irreversible (Fig. S6). The uptake (0.250 mmol g^{-1}) for Pt@HKUST-1/GO is much higher than 0.070 mmol g^{-1} for the same system under the similar temperature and pressure [17], which was prepared by the self-assembly between Pt@GO and precursors of HKUST-1. The repeatability of hydrogen adsorption for Pt@HKUST-1/GO was further confirmed (Fig. S7).

Undoubtedly, the significant enhancement cannot be ascribed to differences in BET values because of the obviously decreased or unchanged values of two composites with respect to MOFs. In fact, the spillover mechanism is responsible for the significant elevation in hydrogen uptakes. Recent studies have shown increased hydrogen uptakes on MOFs by spillover [2,3]. In general, the metal NPs and MOFs act as the spillover sources of hydrogen molecules and receptors, respectively. In our case, hydrogen molecules first chemisorbed and dissociated on the surface of Pt NPs, and then hydrogen atoms migrated and diffuse into the surface and internal pores of the MOF/GO receptor. Spillover effect was still involved in our composites in spite of obvious aggregations of Pt NPs throughout MOF/GO supports.

In conclusion, Pt@MOF/GO composites were synthesized through a colloidal NP incipient-wetness impregnation method. The merit of MOF/GO supports and spillover mechanism was responsible for significantly enhanced hydrogen uptakes at 298 K. Our results show

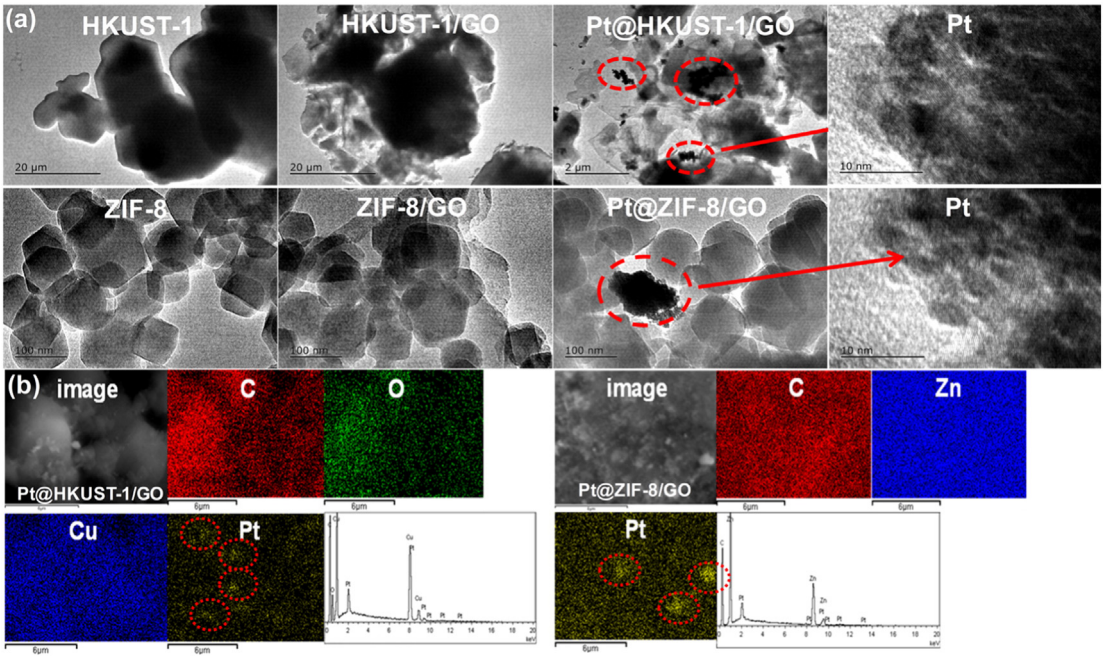

Fig. 1. (a) TEM images, and (b) elemental mapping distribution of Pt@HKUST-1/GO and Pt@ZIF-8/GO systems; red dotted lines represent the aggregated Pt NPs. (For interpretation of the references to color in this figure legend, the reader is referred to the web version of this article.)

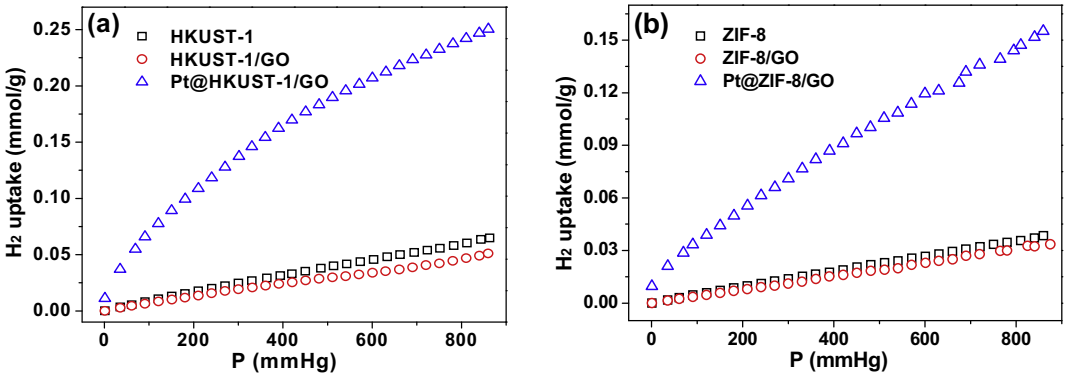

Fig. 2. Hydrogen adsorption isotherms for (a) Pt@HKUST-1/GO, and (b) Pt@ZIF-8/GO systems at 298 K.

that MOF/GO can be developed as excellent supports to incorporate NPs, and the metal-assisted storage via spillover has been shown as a most promising approach for hydrogen storage at ambient temperature. Further studies on searching for effective strategies to control the spatial distribution of metal NPs on supports, and then optimizing the sample preparation are currently in progress in our laboratory.

Acknowledgments

The authors thank the National Natural Science Foundation (51072072, 51102119, 51272095), Natural Science Foundation of Jiangsu Province (BK2011518), Qing Lan Project of Jiangsu Province, China Postdoctoral Science Foundation (2014M561578), and Jiangsu Planned Projects for Postdoctoral Research Funds (1401109C).

Appendix A. Supplementary material

Supplementary data to this article can be found online at http://dx.doi.org/10.1016/j.inoche.2015.02.001.

References

[1] M.P. Suh, H.J. Park, T.K. Prasad, D.W. Lim, Chem. Rev. 112 (2012) 782.
[2] L.F. Wang, A.J. Lachawiec Jr., R.T. Yang, RSC Adv. 3 (2013) 23935.
[3] L.F. Wang, R.T. Yang, Energy Environ. Sci. 1 (2008) 268.
[4] A.J. Robell, E.V. Ballou, M. Boudart, J. Phys. Chem. 68 (1964) 2748.
[5] Y.W. Li, R.T. Yang, J. Am. Chem. Soc. 128 (2006) 726.
[6] Y.W. Li, R.T. Yang, J. Am. Chem. Soc. 128 (2006) 8136.
[7] Y.W. Li, R.T. Yang, Langmuir 23 (2007) 12937.
[8] Y.W. Li, R.T. Yang, AICHE J. 54 (2008) 269.
[9] Y.Y. Liu, J.L. Zeng, J. Zhang, F. Xu, L.X. Sun, Int. J. Hydrog. Energ. 32 (2007) 4005.
[10] C. Petit, T.J. Bandosz, Adv. Mater. 21 (2009) 4753.
[11] C. Petit, J. Burress, T.J. Bandosz, Carbon 49 (2011) 563.
[12] C. Petit, T.J. Bandosz, Adv. Funct. Mater. 21 (2011) 2108.
[13] I. Ahmed, N.A. Khan, S.H. Jhung, Inorg. Chem. 52 (2013) 14155.
[14] S.L. Zhang, Z. Du, G.K. Li, Talanta 115 (2013) 32.
[15] Y. Zhang, G. Li, H. Lu, Q. Lv, Z.G. Sun, RSC Adv. 4 (2014) 7594.
[16] R. Kumar, K. Jayaramulu, T.K. Maji, C.N.R. Rao, Chem. Commun. 49 (2013) 4947.
[17] H. Zhou, X.Q. Liu, J. Zhang, X.F. Yan, Y.J. Liu, A.H. Yuan, Int. J. Hydrog. Energ. 39 (2014) 2160.
[18] J. Zhang, X.Q. Liu, H. Zhou, X.F. Yan, Y.J. Liu, A.H. Yuan, RSC Adv. 4 (2014) 28908.
[19] W.S. Hummers, R.E. Offeman, J. Am. Chem. Soc. 80 (1958) 1339.
[20] Y. Wang, J.W. Ren, K. Deng, L.L. Gui, Y.Q. Tang, Chem. Mater. 12 (2000) 1622.
[21] A.R. Millward, O.M. Yaghi, J. Am. Chem. Soc. 127 (2005) 17998.
[22] J. Cravillon, S. Münzer, S.J. Lohmeier, A. Feldhoff, K. Huber, M. Wiebcke, Chem. Mater. 21 (2009) 1410.
[23] S.S.Y. Chui, S.M.F. Lo, J.P.H. Charmant, A.G. Orpen, I.D. Williams, Science 283 (1999) 1148.
[24] K.S. Park, Z. Ni, A.P. Côté, J.Y. Choi, R. Huang, F.J. Uribe-Romo, H.K. Chae, M. O Keeffe, O.M. Yaghi, Proc. Natl. Acad. Sci. U. S. A. 103 (2006) 10186.
[25] D.Y. Cai, M. Song, J. Mater. Chem. 17 (2007) 3678.
[26] B. Panella, M. Hirscher, H. Pütter, U. Müller, Adv. Funct. Mater. 16 (2006) 520.